ResearchGate

See discussions, stats, and author profiles for this publication at: https://www.researchgate.net/publication/6175293

An RNAi-based genetic screen for oxidative stress resistance reveals retinol saturase as a mediator of stress resistance

ARTICLE *in* FREE RADICAL BIOLOGY AND MEDICINE · OCTOBER 2007

Impact Factor: 5.74 · DOI: 10.1016/j.freeradbiomed.2007.05.008 · Source: PubMed

CITATIONS
14

READS
45

5 AUTHORS, INCLUDING:

Naoki Matsuo
Osaka University
16 PUBLICATIONS **1,034** CITATIONS
SEE PROFILE

Brian Lee Perkins
Swansea University
5 PUBLICATIONS **206** CITATIONS
SEE PROFILE

Clara Limbaeck-Stokin
University of Ljubljana
7 PUBLICATIONS **93** CITATIONS
SEE PROFILE

Mark Mayford
The Scripps Research Institute
57 PUBLICATIONS **6,950** CITATIONS
SEE PROFILE

All in-text references underlined in blue are linked to publications on ResearchGate, letting you access and read them immediately.

Available from: Brian Lee Perkins
Retrieved on: 24 January 2016

Available online at www.sciencedirect.com
ScienceDirect
Free Radical Biology & Medicine 43 (2007) 781–788
www.elsevier.com/locate/freeradbiomed

Original Contribution

An RNAi-based genetic screen for oxidative stress resistance reveals retinol saturase as a mediator of stress resistance

Rie Nagaoka-Yasuda [a,b], Naoki Matsuo [a], Brian Perkins [a], Klara Limbaeck-Stokin [a,c], Mark Mayford [a,*]

[a] *Department of Cell Biology, The Scripps Research Institute, 10550 North Torrey Pines Road, La Jolla, CA 92037, USA*
[b] *Department of Pharmacological Sciences, Musashino University, Nishi-Tokyo 202-8585, Japan*
[c] *Institute of Pathology, Faculty of Medicine, University of Ljubljana, Ljubljana, Slovenia*

Received 15 December 2006; revised 6 April 2007; accepted 10 May 2007
Available online May 16 2007

Abstract

Oxidative stress has been implicated in the pathogenesis of numerous late-onset diseases as well as organismal longevity. Nevertheless, the genetic components that affect cellular sensitivity to oxidative stress have not been explored extensively at the genome-wide level in mammals. Here we report an RNA interference (RNAi) screen for genes that increase resistance to an organic oxidant, *tert*-butylhydroperoxide (*tert*-BHP), in cultured fibroblasts. The loss-of-function screen allowed us to identify several short hairpin RNAs (shRNAs) that elevated the cellular resistance to *tert*-BHP. One of these shRNAs strongly protected cells from *tert*-BHP and H_2O_2 by specifically reducing the expression of retinol saturase, an enzyme that converts all-*trans*-retinol (vitamin A) to all-*trans*-13,14-dihydroretinol. The protective effect was well correlated with the reduction in mRNA level and was observed in both primary fibroblasts and NIH3T3 cells. The results suggest a novel role for retinol saturase in regulating sensitivity to oxidative stress and demonstrate the usefulness of large-scale RNAi screening for elucidating new molecular pathways involved in stress resistance.
© 2007 Elsevier Inc. All rights reserved.

Keywords: Stress resistance; RNA interference; Genetic screen; Oxidative stress; *tert*-Butylhydroperoxide; Free radicals

Genetic screens in invertebrates such as *Caenorhabditis elegans* have been successful in identifying mutant animals with significant increases in longevity and have guided the exploration for novel genetic components involved in mammalian aging. It is impractical to apply similar screens to mammals, given their relatively long average life span; however, there is a clear link between increased stress resistance and life-span extension in invertebrates [1]. Recent studies have suggested that the link is conserved in mammals [2–5]. Related studies have also demonstrated that fibroblasts isolated from mutant mice with extended life span exhibit an increased resistance to multiple oxidative stresses in vitro [3,6,7], suggesting that a genetic screen for fibroblasts with increased stress resistance may be useful for elucidating new molecular pathways involved in mammalian aging and age-related disorders.

RNA interference (RNAi) is an emerging tool that enables the suppression of gene function without modifying genomic DNA sequences [8,9]. This technique is especially beneficial when combined with cell-based genetic screens, as previous mutagenesis was unable to generate recessive phenotypes in the cultured cells due to the diploid nature of somatic cells [10]. RNAi screens of mammalian cells have proved their worth in the identification of novel tumor suppressors, regulators of cell division, and components of protein degradation [11–13].

Here we designed a cell-based RNAi screen for increased resistance to oxidative stress. We used a biochemical approach

Abbreviations: HEK, human embryonic kidney; RNAi, RNA interference; shRNA, short hairpin RNA; *tert*-BHP, *tert*-butylhydroperoxide; GAPDH, glyceraldehyde-3-phosphate dehydrogenase; RetSat, retinol saturase; UV, ultraviolet; ER, endoplasmic reticulum; IP3K1, inositol 1,4,5-triphosphate kinase 1; 4-HNE, 4-hydroxynonenal; PLD3, phospholipase D3; CPABP, cytoplasmic poly(A) binding protein 3; pdcd7, programmed cell death protein 7; NADH, nicotinamide adenine dinucleotide; NADPH, nicotinamide adenine dinucleotide phosphate.

* Corresponding author. Fax: +1 858 784 9860.
E-mail address: mmayford@scripps.edu (M. Mayford).

0891-5849/$ - see front matter © 2007 Elsevier Inc. All rights reserved.
doi:10.1016/j.freeradbiomed.2007.05.008

to generate a highly complex short hairpin RNA (shRNA) library from an arrayed cDNA library (NIA 15K). The uniquely high complexity of the shRNA library, more than 10^6 independent clones, ensures a range of knockdown levels for each gene represented. We used retroviral base delivery of the library to select several shRNAs that protect cultured fibroblasts from *tert*-butylhydroperoxide (*tert*-BHP) and H_2O_2. A shRNA targeting retinol saturase, an enzyme that converts vitamin A (all-*trans*-retinol) into a novel retinoid, produced the strongest resistance. The resistance was specific to peroxide-induced damage and quantitatively related to the degree of retinol saturase silencing. These results suggest an unexpected link between retinoid metabolism and cellular resistance to oxidative stress. This approach should prove generally useful in identifying novel signaling pathways involved in stress resistance.

Materials and methods

Cell culture and retroviral infection

NIH3T3 cells were maintained in DMEM supplemented with 10% calf serum, and human embryonic kidney (HEK) 293 cells were grown in DMEM supplemented with 10% fetal bovine serum. Mouse primary fibroblasts were dissociated from tail skin by incubation in a digestion mixture (0.025% collagenase, 0.025% dispase, and 0.5% trypsin with 1 mM $CaCl_2$) with vigorous shaking at 37°C for 1 h. The remaining clumps were removed by filtration, and resultant single cells were maintained in DMEM supplemented with 10% fetal bovine serum. For virus production, HEK293 cells were cotransfected with the ecotropic packaging vector pCL-Eco and an RNAi library in the psiRNA3 vector or with a pSupressor-Retro vector encoding designed shRNAs by the calcium phosphate method. Viral transduction was performed by incubating host cells (NIH3T3 cells or primary fibroblasts) in viral supernatant diluted with fresh medium at a dilution of 1:1 in the presence of 8 μg/ml Polybrene. Infection efficiency was monitored by GFP expression at 48 h after the initial infection for the library transduction and by G418 resistance for pSupressorRetro infection. Cell growth was monitored by cell counting with trypan blue exclusion.

shRNA library construction

To generate a highly complex shRNA library we began with the NIA 15K arrayed cDNA library [14]. Individual clones were grown, plasmid DNA was prepared and pooled, and the cDNA inserts were isolated from the vector. Partial digestion with DNase I was calibrated to obtain fragments in the 20–25 bp range. This was achieved by digesting 10 μg cDNA with 0.2 U DNase I for 25 min at 15°C in reaction buffer containing 50 mM NaCl. The reaction was stopped with EDTA and phenol extraction, followed by spinning in G25 spin columns (buffer contained 50 mM NaCl throughout). Blunt ends were generated with T4 DNA polymerase, and the samples were ligated with oligo pairs A and B in a 10-fold molar excess. Ligated DNA was size-fractionated on a 3% Agarose1000 gel, and DNA in the 113–121 bp size range was purified. The size-fractionated DNA was amplified by PCR using Taq polymerase and primers AP and BP (amplification was for 15–20 cycles to be certain the reaction was within the linear range for amplification). The sample was digested with FokI and ligated with a 5-fold molar excess of oligo D (hairpin oligo). The sample was then digested with HinfI and fractionated on a 3% Agarose1000 gel, and fragments in the 48–60 bp range were purified. The purified hairpin fragments were ligated with oligo C and subjected to hairpin PCR using primers E and F. The reaction mixture consisted of 300 μM dNTPs, 25 pM oligos, 5 μl ligation mix, and 2 μl VENT (exo-) in a 100-μl volume in the recommended buffer. PCR was for 12 cycles: 95°C for 3 min, 95°C for 30 s, 63°C for 3 min, 72°C. The number of PCR cycles was adjusted to be within the linear range of amplification. The amplified product (ca. 210 bp) was digested in series with MboII, FokI, MlyI, and MspI and ligated with a 10-fold molar excess of oligos K, M1, and M2 and then ligated into psiRNA3 carrying the U6 promoter. The resultant plasmids were then introduced into *Escherichia coli.* The library comprised 1.4×10^6 independent clones.

RNA interference screen

NIH3T3 cells were infected with the shRNA library three times for 6–8 h each with 6- to 8-h intervals during which the cells were incubated in fresh culture medium. Transduced cells were cultured for 3 days after the final retrovirus exposure and then exposed to 400 μM *tert*-BHP (Sigma) for 2 h. The surviving cells were expanded at 20% confluence or higher for 2 weeks and exposed to 400 μM *tert*-BHP. Genomic DNA was isolated from the surviving cells using conventional methods. Retroviral inserts were recovered by PCR with primers against a sequence within the psiRNA3 vector (siseq1, 5′-CTGTAGGTTTGGCAAGCTAGC-3′, siseq2, 5′-AGGGTCATTTCAGGTCCTTGG-3′). SalI–BstXI fragments of the PCR products were subcloned into psiRNA3 to generate an enriched library for sequence analysis or a second round of screening. For the second round of screening, HEK293 cells were cotransfected with the enriched library and the packaging vector. To lower m.o.i., parental NIH3T3 cells were exposed to the viral supernatant for only 2 h and subjected to further selection with 400 μM *tert*-BHP.

Retroviral vectors for expressing the three shRNAs against retinol saturase

Short hairpin sequences were designed using a program from the G. Hannon lab (http://katahdin.cshl.org%3A9331/homepage/SiRNA/). The shRNAs were constructed according to the manufacturer's protocol for the pSuppressorRetro vector (IMGENEX). Briefly, the respective forward and reverse primers at 50 μg/ml were annealed, treated with polynucleotide kinase, and subcloned into SalI–XbaI sites of pSuppressorRetro. All constructs were verified by sequencing throughout the hairpin region. The forward primers were for si-49, 5′-TCGACTGTCCTCCCTCCTACAGCAGACTCCTGTGC

TGTAGGAGGGAGGACATTTTT-3′; for si-70, 5′-TCGACTGGTTGCACATATAAACAAGACTCCTGTTGTTTATATGTGCAAGGATTTTT-3′; and for si-65, 5′-TCGACGCAATTCCTTGCACATATAGACTCCTGTATATGTGCAAGGAATTGCTTTTT-3′. The reverse primers were for si-49, 5′-CTAGAAAAATGTCCTCCCTCCTACAGCACAGGAGTCTGCTGTAGGAGGGAGGACAG-3′; for si-70, 5′-CTAGAAAAATCCTTGCACATATAAACAACAGGAGTCTTGTTTATATGTGCAAGGAG-3′; and for si-65, 5′-CTAGAAAAAGCAATTCCTTGCACATATACAGGAGTCTATATGTGCAAGGAATTGCG-3′.

Northern blotting

Northern blots were conducted using total RNA purified by Trizol-LS (Invitrogen). Twenty micrograms of total RNA was fractionated on a 1.0% formaldehyde–agarose gel and transferred to a Zeta-Probe membrane (Bio-Rad) in 10× SSC. Hybridization was performed at 65°C with ^{32}P-labeled probes in PerfectHyb Plus hybridization buffer (Sigma). The membranes were washed twice at 65°C in 2× SSC for 10 min, twice at 65°C in 1× SSC for 10 min, and twice at 65°C in 0.1× SSC for 10 min. Probes for retinol saturase were generated by labeling a BamHI fragment from the cDNA clone from the NIA-15K cDNA library (H3045H-01) with [^{32}P]dCTP. Template DNA for glyceraldehyde-3-phosphate dehydrogenase (GADPH) was purchased from Amnion, Inc.

Cytotoxicity assay

Cells were seeded in 96-well plates at a density of 4×10^3 per well at 24 h before treatments and were then exposed to various doses of *tert*-BHP or H_2O_2 for 2 h. For UVC treatment, culture medium was replaced with 100 μl of PBS, and cells were irradiated in a UVC light box (Stratalinker, 254 nm; Stratagene). After the irradiation, the PBS was replaced with normal culture medium. Methyl viologen dichloride hydrate (Paraquat; Sigma) was dissolved in culture medium and added to the culture until cell viability was measured. Three replicate wells were used for each dose of *tert*-BHP, H_2O_2, UVC radiation, and paraquat. For the MTT assay, the culture medium was replaced with 100 μl fresh medium containing 1 mg/ml 3-(4,5-dimethylthiazol-2-yl)-2,5-diphenyltetrazolium bromide (Sigma) in each well, and the plates were incubated for an additional 4 h at 37°C. After the medium was removed, intracellular formazan dye crystals were dissolved in 100 μl of DMSO, and the absorbance of formazan at 562 nm was measured using a plate reader.

Microarray analysis

Total RNA was isolated from cells with empty retroviral vector or the vector encoding si-RetSat by using Trizol-LS (Invitrogen). RNA probes were generated by in vitro transcription and hybridized with the GeneChip Mouse Genome 430 2.0 Array (Affymetrix) according to the manufacturer's protocol.

Results

To construct a shRNA library with high complexity from a mouse cDNA library, we used an enzymatic production method. Briefly, individual clones from the NIA 15K arrayed cDNA library were grown, plasmid DNA was prepared and pooled, and the cDNA inserts were isolated from the vector. Partial digestion with DNase I was calibrated to obtain fragments in the 20–25 bp range, and hairpin sequences were generated by a combination of hairpin PCR and digestion with restriction enzymes. The generated short hairpin sequences (corresponding to 1.4×10^6 independent colonies) were expressed under the U6 promoter in a retrovirus-based expression vector (psiRNA3). To produce ecotropic retrovirus, HEK293 cells were cotransfected with the retroviral RNAi library and a packaging vector (pCL-Eco). To achieve maximum delivery of the library to NIH3T3 cells, fresh viral supernatant was diluted and added repeatedly to 7.5×10^5 NIH3T3 cells (Fig. 1). Under these conditions, the infection levels, assessed by the GFP signal, approached 100%. To screen for cells that were resistant to lethal oxidative stress, a prototypical organic oxidant, *tert*-BHP, was used. This agent is widely used to study oxidative damage in a variety of cell types [15–17]. The infected NIH3T3 cells were expanded for 3 days and exposed to 400 μM *tert*-BHP for 2 h. Cell survival, determined by trypan blue exclusion, was less than 0.5% after this treatment (Table 1). The surviving cells were expanded and a second *tert*-BHP selection was performed 2 weeks after the initial treatment. Although cell viability was slightly higher (approximately 1.0%), there was no enrichment for particular shRNAs at this point, as determined by sequence analysis of retroviral inserts amplified from the genomic DNA of the surviving cells (Table 2).

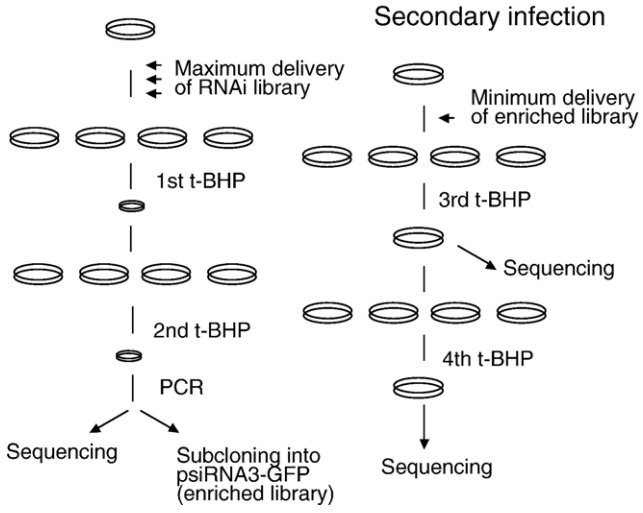

Fig. 1. Screening scheme for the enrichment of shRNAs that elevate cellular resistance to *tert*-BHP. The RNAi library was introduced into NIH3T3 cells by retroviral infection. Transduced cells were selected for *tert*-BHP resistance (400 μM for 2 h) twice. Viral inserts encoding shRNAs were recovered by PCR from the genomic DNA of the surviving cells after the second *tert*-BHP selection, cloned into the psiRNA3 vector (an enriched library), and used for a secondary infection of NIH3T3 cells. After each of two additional *tert*-BHP selections, the viral inserts were recovered by PCR and sequenced.

Table 1
Increase in viability of cells transduced with the RNAi library

tert-BHP selection	Cell viability (%)	
	Empty vector	RNAi library
First	N/D	0.2
Second	N/D	1.0
Third	2.0	14.0
Fourth	0.6	15.5

To further enrich the shRNAs that promote cell survival after the *tert*-BHP treatment, we performed a second round of selection. Retroviral inserts recovered from the first round of selection were subcloned into the viral expression vector psiRNA3 (enriched library). To avoid multiple infections, parental NIH3T3 cells were exposed to the enriched library for a short time. The infected cells were again expanded and exposed to a third, and in some cases a fourth, *tert*-BHP treatment, and viability was monitored in parallel by comparison with cells infected with an empty vector (Table 1). Whereas only 2% of the cells carrying empty vector survived the third *tert*-BHP treatment, 14% of the cells infected with the enriched RNAi library were viable. This elevation in cell viability was also seen at the fourth *tert*-BHP treatment; 0.6% of the cells with empty vector survived, whereas 15.5% of the cells transfected with the enriched library were viable.

Table 2
Analysis of RNAi library inserts amplified from NIH3T3 cells after *tert*-BHP selection

Sequence homology	Accession No.	No. of clones after *tert*-BHP selection		
		Second	Third	Fourth
3′ UTR of retinol saturase	AK002851	0	27	9
Phospholipase D	NM_011116	1	5	0
Cell death protein 7	BC022772	1	1	0
POU domain, class 2 transcription factor 3	NM_011139	2	0	0
3′ UTR of unc-51-like kinase 1	NM_009469	1	0	0
Similar to glutathione synthetase ATP binding domain	AK016577	1	0	0
3′ UTR of cytoplasmic polyadenylation element binding protein 3 (CPEB)	AK147243	0	2	0
CDS and 3′ UTR of cysteine conjugate-β lyase 1	BC052047	0	1	0
Ribosomal protein L7a	BC029992	0	1	0
3′ UTR of junction adhesion molecule 3	NM_023277	0	1	0
20S proteasome subunit C2 (PsmaI)	NM_011965	0	1	0
Unknown 3 (508, 515, 545)	AC123618	0	3	0
Unknown2 (537)	AC100927	0	1	0
Unknown 1 (501)	AC139131	0	1	0
Cystatin 8	NM_009978	0	0	1
Unable to read [a]		1	4	0
No hairpin [b]		2	15	2
Total		9	64	12

[a] Hairpin sequences with more than 7N were considered as clones that were unable to be sequenced.

[b] Viral inserts without hairpin sequence between the U6 promoter and the termination signal were considered as no hairpins.

To identify the shRNAs responsible for the increased resistance to *tert*-BHP, retroviral inserts were cloned and sequenced (Table 2). The most abundant clone encoded a 21-bp shRNA complementary to the 3′ UTR of mouse retinol saturase (si-RetSat), an enzyme that catalyzes the production of a novel retinoid derivative, all-*trans*-13,14-dihydroretinol, from all-*trans*-retinol (vitamin A) [18]. Significant enrichment of si-RetSat was confirmed after the fourth *tert*-BHP selection (Table 2). We also identified shRNAs for phospholipase D3 (si-PLD3) and programmed cell death protein 7 (si-pdcd7), at both the second and the third *tert*-BHP selections. An shRNA for cytoplasmic poly(A) element binding protein (si-CPABP) was detected twice at the third selection. We further tested these shRNAs individually for their ability to increase *tert*-BHP resistance.

We examined the effects of candidate shRNAs on *tert*-BHP resistance in mouse primary fibroblasts. Primary fibroblasts isolated from adult mouse tails were infected with empty psiRNA3 or vector encoding si-CPABP, si-pdcd7, si-PLD3, or si-RetSat. *tert*-BHP (50 μM) was applied for 2 h, and cell viability was quantified 48 h after treatment. As shown in Fig. 2, the expression of si-RetSat induced a prominent increase in the viability of primary fibroblasts exposed to *tert*-BHP. A significant increase in cell viability relative to empty vector controls was also observed with si-PLD3 and si-CPABP. Similar protective effects were observed when a higher dose of *tert*-BHP (100 μM) was applied (data not shown).

When si-RetSat was expressed in NIH3T3 cells, its protective effect on *tert*-BHP-induced cytotoxicity was dramatic. As shown in Fig. 3A, cells expressing si-RetSat were barely damaged 24 h after exposure to 400 μM *tert*-BHP, whereas cells with the empty vector were almost completely killed by the same treatment. Notably, there was little difference in cell morphology (Fig. 3A) or growth rate between the cells

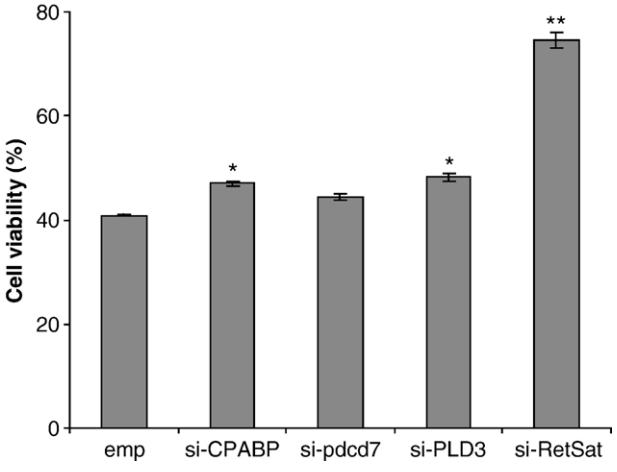

Fig. 2. Effects of candidate shRNAs on *tert*-BHP resistance in the primary fibroblasts. Individual shRNAs isolated from the screen (si-CPABP, si-pcdc7, si-PLD3, and si-RetSat) were introduced into primary fibroblasts at passage 2. The infected cells were exposed to 50 μM *tert*-BHP for 2 h, and cell viability was examined by the MTT method 48 h after the exposure. Error bars represent SD of the means. Post hoc test showed significance for si-CAPBP ($p<0.05$), si-PLD3 ($p<0.05$), and si-RetSat ($p<0.01$).

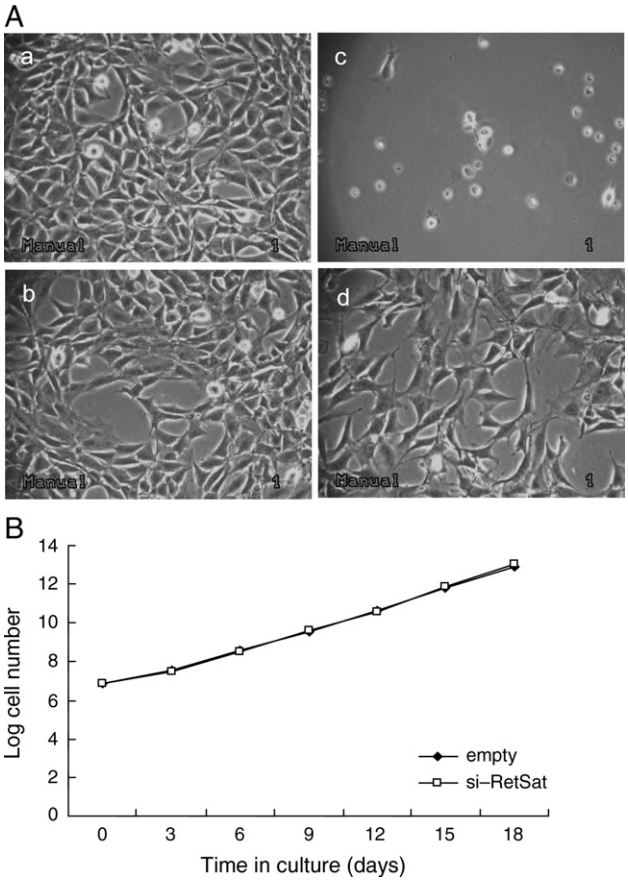

Fig. 3. Protective effect of si-RetSat on *tert*-BHP toxicity does not affect cell morphology or growth rate under normal conditions. (A) NIH3T3 cells were transduced with empty vector (a and c) or pSuppressorRetro encoding si-RetSat (b and d) and exposed to 400 μM *tert*-BHP for 2 h. Phase-contrast images were taken before (a and b) or 24 h after (c and d) the treatment. (B) Normal proliferation of NIH3T3 cells expressing shRNAs for retinol saturase. Growth rate was monitored by cell counting with trypan blue exclusion every 3 days for 18 days.

expressing empty vector and those expressing si-RetSat over 10 passages (Fig. 3B).

Retinol saturase has been characterized as an enzyme that regulates retinoid metabolism [18,19]; however, its involvement in the cytotoxic response to oxidative stress has not been reported. To determine whether si-RetSat suppresses mRNA for retinol saturase, we made Northern blots from cells transfected with si-RetSat or empty vector and probed them for retinol saturase. As shown in Fig. 4A, a 2.2-kb transcript, identical in size to that of mouse retinol saturase mRNA, was detected in NIH3T3 cells transfected with the empty vector, whereas the mRNA signal from this band was decreased to 16% of control levels in cells expressing si-RetSat.

We examined the specificity of si-RetSat by expressing shRNAs targeting different retinol saturase sequences near the RNA sequence targeted by si-RetSat (si-49, si-70, si-65). Northern blotting revealed that the expression of si-49, si-70, and si-65 induced 40, 36, and 65% reductions in retinol saturase mRNA, respectively (Fig. 4A). Whereas all four shRNAs enhanced the cell survival from *tert*-BHP treatment, greater protective effects were observed at higher levels of retinol saturase mRNA suppression (Fig. 4B). Thus, there was a tight correlation between decreases in retinol saturase mRNA levels and increased cellular resistance to *tert*-BHP.

The specific suppression of retinol saturase by si-RetSat was also supported by microarray analysis. There was little difference in the expression levels of 39,000 mouse transcripts between the cells expressing si-RetSat and those expressing empty vector (Fig. 5A). The correlation coefficients of the relative gene expression levels in the two groups approached 1.0 (0.992 for experiment 1 and 0.994 for experiment 2), and the number of genes that scored as "differentially expressed" based on the two independent comparisons was small (10 decreases and 13 increases, all with a less than 2.0-fold change). These results suggest that retinol saturase is the specific target of si-RetSat and that the suppression of retinol saturase does not lead

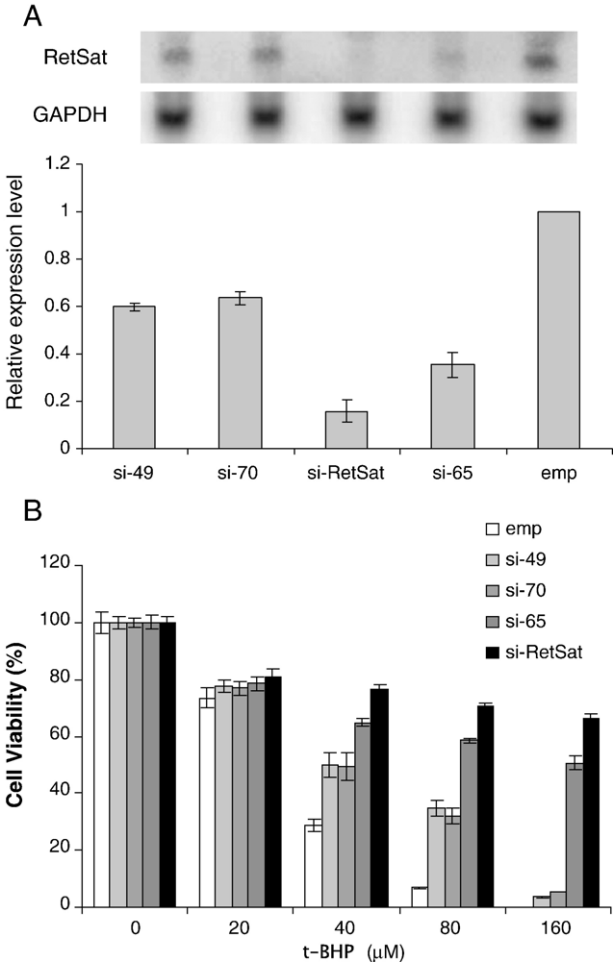

Fig. 4. Suppression of retinol saturase mRNA and increased resistance to *tert*-BHP induced by shRNAs targeting different regions of the retinol saturase gene. (A) Total RNA was isolated from NIH3T3 cells expressing shRNAs targeting retinol saturase (si-49, si-70, si-RetSat, or si-65) and cells containing empty vector (emp) and subjected to a Northern blot analysis for retinol saturase and GAPDH expression (top). The hybridization signal was quantified by a phosphoimager. Error bars represent SD of the means. (B) Protection of cells from a wide range of *tert*-BHP exposure. NIH3T3 cells expressing si-49, si-70, si-RetSat, or si-65 or carrying empty vector were exposed to the indicated dose of *tert*-BHP for 2 h, and cell viability was examined at 72 h after treatment using a MTT assay. Error bars represent SD of the means. Post hoc test showed significance for all the siRNAs at concentrations greater than 40 μM.

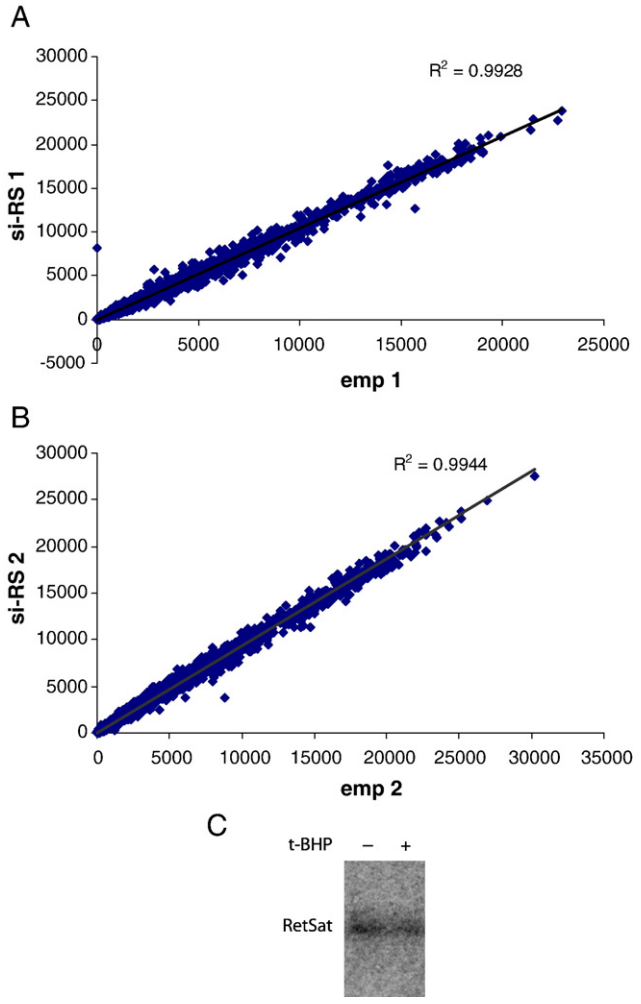

Fig. 5. Highly similar expression profiles of NIH3T3 cells expressing empty vector and si-RetSat. (A) Total RNA was isolated from exponentially growing cells 2 weeks after the retroviral infection and analyzed on MOE 430 Affymetrix mouse expression arrays. Relative expression levels of genes expressed in the cells containing si-RetSat and empty vector are plotted on the *y* and *x* axes, respectively. Correlation coefficients are indicated as R^2. Two independent comparisons were performed, using independent total RNA preparation. (B) Lack of transcriptional induction of retinol saturase. Total RNA was isolated from NIH3T3 cells before and after 30 min exposure to 400 μM *tert*-BHP and subjected to a Northern blot analysis for retinol saturase.

to major changes in the global transcription profile. We further examined mRNA levels of retinol saturase with or without *tert*-BHP exposure by Northern blotting (Fig. 5B). There was no significant induction of retinol saturase at 30 min after the exposure, suggesting that the increased resistance to *tert*-BHP is caused by constitutive suppression of retinol saturase.

We next asked whether the expression of si-RetSat protects cells from other forms of oxidative stress. First, we examined H_2O_2-induced cytotoxicity (Fig. 6A), because it causes oxidative damage similar to that induced by *tert*-BHP. As expected, NIH3T3 cells expressing any of the shRNAs targeting retinol saturase showed elevated resistance to H_2O_2, although the effect was smaller than when assayed using *tert*-BHP. The resistance again correlated with the level of suppression of retinol saturase mRNA levels. The suppression of retinol saturase expression had little effect on cell death induced by either UV or paraquat (Figs. 6B and 6C).

Discussion

In the present study, we performed a cell-based screen for RNAi that increased resistance to oxidative stress. By enriching

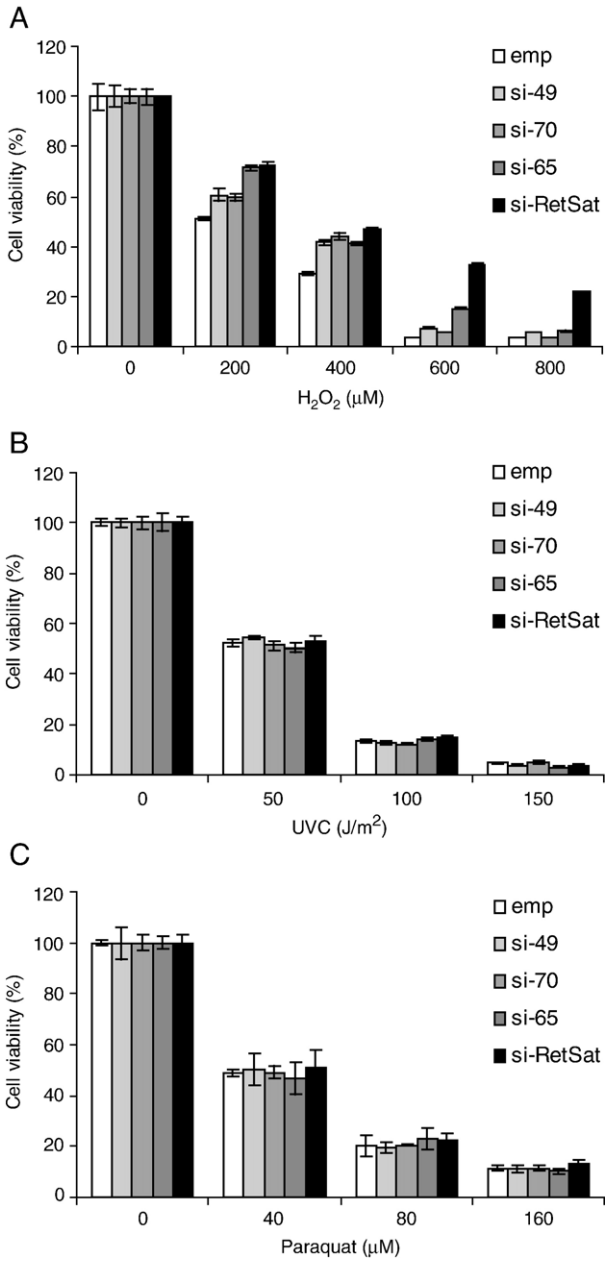

Fig. 6. Effect of retinol saturase suppression on the cellular response to H_2O_2, UVC, and paraquat. NIH3T3 cells expressing si-49, si-70, si-RetSat, si-65, or empty vector were exposed to the indicated dose of (A) H_2O_2, (B) UVC, or (C) paraquat. Cell viability was examined at 2 days after the H_2O_2 and UV exposures and at 5 days after paraquat exposure using an MTT assay. Post hoc test showed a significant improvement in survival for si-49, si-65, and si-RetSat at concentrations greater than 200 μM H_2O_2 and for si-70 at 200, 400, and 800 μM H_2O_2. No significant change in cell viability was observed when the same cells were exposed to UVC or paraquat. Error bars represent SD of the means.

for transfected fibroblasts that survived repeated exposure to a lethal dose of *tert*-BHP, we have identified shRNAs that enhance cellular resistance to *tert*-BHP in vitro. We further characterized one of the putative targets, retinol saturase, by designing shRNAs with varying suppression efficiencies and found that cellular resistance to *tert*-BHP and H_2O_2 increased as retinol saturase was progressively suppressed. RNA profiling indicated that there was no prominent alteration in the expression of any of the 39,000 transcripts represented on the microarray. Furthermore, there was no immediate (30 min after the addition of *tert*-BHP) induction of retinol saturase transcription upon *tert*-BHP exposure in wild-type cells (Fig. 5B). These results strongly suggest that the constitutive reduction in retinol saturase by the RNAi is the primary cause of the elevated cellular resistance to oxidative stress.

Despite their potent protective effects against *tert*-BHP and H_2O_2-induced cytotoxicity, the same siRNAs had little impact on cell survival after UV radiation or paraquat exposure, which generate free radical damage by different mechanisms. UV uses a variety of signaling pathways, involving nuclear DNA damage as a predominant pathway, because experimental reduction of DNA damage is associated with a loss of these effects [20]. The mechanisms of paraquat toxicity involve the generation of superoxide anions through the process of redox cycling [21], which requires several days to damage fibroblasts, whereas *tert*-BHP and H_2O_2 induce cell death within 24 h of exposure. Thus, retinol saturase seems to selectively affect cell sensitivity to an acute rise in peroxide-generated free radicals. Previous studies have shown that *tert*-BHP and/or H_2O_2 triggers a number of reactions, including peroxidation of membrane lipids, oxidation of glutathione, loss of protein thiols, elevation of cytosolic Ca^{2+}, loss of endoplasmic reticulum (ER) stress proteins, and increased mitochondrial permeability [15–17,22–24]. Ca^{2+} release from the ER may be relatively specific to *tert*-BHP and H_2O_2-induced cell death, given that similar selective resistance is reported in a *Drosophila* mutant lacking inositol 1,4,5-triphosphate kinase I (IP3K1). IP3K1 binds to the IP3 receptor and triggers Ca^{2+} release from the ER [25]. The mutation protects *Drosophila* from H_2O_2 toxicity but not from paraquat, suggesting that Ca^{2+} release from the ER is not required for paraquat-induced cell death. The importance of Ca^{2+} from the ER in *tert*-BHP-induced cytotoxicity is also supported by a study showing that overexpression of an ER stress protein, calreticulin, prevents *tert*-BHP-induced cell death by blocking increases in intracellular Ca^{2+} [16]. Retinol saturase is localized to the ER in transfected HEK293 cells and the membrane fractions of a variety of tissues, suggesting a possible role in these ER-based stress mechanisms [18].

The fibroblast resistance phenotype may also manifest as an interesting organismal aging phenotype. Of seven longevity mutations in mice, at least four are reported to cause increased resistance to oxidative stress in fibroblasts isolated from the mutants [2,3,6,7]. In addition, an abnormal oxidative response is observed in fibroblasts isolated from patients with neurodegenerative diseases. It has been reported that skin fibroblasts taken from patients with Alzheimer disease (AD) shows increased accumulation of the lipoperoxidation products malondialdehyde and 4-hydroxynonenal (4-HNE) compared to controls [26]. Another study demonstrated that 4-HNE exposure induced a larger increase in intracellular ROS levels in AD fibroblasts than in control fibroblasts [27]. In fibroblasts from Down syndrome donors, an imbalance in the activity of the enzymatic antioxidants copper–zinc superoxide dismutase and glutathione peroxidase 1 has been reported [28]. Retinol saturase is expressed ubiquitously, including in brain, and it will be interesting to determine the effect of deleting this gene in other cell types and at the organismal level.

Our screen also suggested that suppression of PLD3, CPABP, and pdcd7 may protect cultured fibroblasts from *tert*-BHP. Some PLDs are reported to mediate angiotensin II-dependent H_2O_2 generation in concert with NADH/NADPH oxidase in vascular smooth muscle cells from hypertensive patients [29]. CPABP is a highly conserved, sequence-specific RNA-binding protein that binds to the cytoplasmic polyadenylation element and modulates translational repression and mRNA localization [30]. In human oocytes, maturation-specific polyadenylation of mRNAs for the enzymatic antioxidants Mn-superoxide dismutase and glutathione peroxidase has been suggested [31]. pdcd7 is characterized as being induced by staurosporine and C2-ceramide-induced apoptosis in T cell thymoma [32]. The same study has also demonstrated that overexpression of pdcd7 increases apoptotic cell death in mouse T cell lymphoma. Those studies suggest potential mechanisms for PLD3, pdcd7, or CPABP in the modulation of cellular resistance to oxidative stress.

In conclusion, we have isolated several shRNAs that confer increased resistance to *tert*-BHP and identified novel modulators of the resistance phenotype. We have confirmed in detail the strongest candidate and shown that the basal levels of retinol saturase expression are inversely correlated with resistance to oxidative stress in fibroblasts. These results suggest an unexpected link between retinoid metabolism and stress resistance. The approach should be generally useful for identifying new molecular pathways in oxidative stress resistance.

Acknowledgments

This work was supported by funds from the Ellison Memorial Foundation to M.M. We thank Dr. Hiromi Takano-Ohmuro for her comments on the manuscript.

References

[1] Finkel, T.; Holbrook, N. J. Oxidants, oxidative stress and the biology of ageing. *Nature* **408:**239–247; 2000.

[2] Holzenberger, M.; D.J.; Ducos, B.; Leneuve, P.; Geloen, A.; Even, P. C.; Cervera, P.; Le Bouc, Y. IGF-1 receptor regulates lifespan and resistance to oxidative stress in mice. *Nature* **421:**182–187; 2003.

[3] Migliaccio, E.; Giorgio, M.; Mele, S.; Pelicci, G.; Reboldi, P.; Pandolfi, P. P.; Lanfrancone, L.; Pelicci, P. G. The p66shc adaptor protein controls oxidative stress response and life span in mammals. *Nature* **402:**309–313; 1999.

[4] Schriner, S. E.; Linford, N. J.; Martin, G. M.; Treuting, P.; Ogburn, C. E.; Emond, M.; Coskun, P. E.; Ladiges, W.; Wolf, N.; Van Remmen, H.; Wallace, D. C.; Rabinovitch, P. S. Extension of murine life span by

overexpression of catalase targeted to mitochondria. *Science* **308:** 1909–1911; 2005.

[5] Yamamoto, M.; Clark, J. D.; Pastor, J. V.; Gurnani, P.; Nandi, A.; Kurosu, H.; Miyoshi, M.; Ogawa, Y.; Castrillon, D. H.; Rosenblatt, K. P.; Kuro-o, M. Regulation of oxidative stress by the anti-aging hormone klotho. *J. Biol. Chem.* **280:**38029–38034; 2005.

[6] Murakami, S.; Salmon, A.; Miller, R. A. Multiplex stress resistance in cells from long-lived dwarf mice. *FASEB J.* **17:**1565–1566; 2003.

[7] Salmon, A. B.; Murakami, S.; Bartke, A.; Kopchick, J.; Yasumura, K.; Miller, R. A. Fibroblast cell lines from young adult mice of long-lived mutant strains are resistant to multiple forms of stress. *Am. J. Physiol. Endocrinol. Metab.* **289:**E23–E29; 2005.

[8] Fire, A.; Xu, S.; Montgomery, M. K.; Kostas, S. A.; Driver, S. E.; Mello, C. C. Potent and specific genetic interference by double-stranded RNA in Caenorhabditis elegans. *Nature* **391:**806–811; 1998.

[9] Elbashir, S. M.; Harborth, J.; Lendeckel, W.; Yalcin, A.; Weber, K.; Tsuchl, T. Duplexes of 21-nucleotide RNAs mediate RNA interference in cultured mammalian cells. *Nature* **411:**494–498; 2001.

[10] Paddison, P. J.; Hannon, G. J. RNA interference: the new somatic cell genetics? *Cancer Cell* **2:**17–23; 2002.

[11] Berns, K.; Hijmans, E. M.; Mullenders, J.; Brummelkamp, T. R.; Velds, A.; Heimerikx, M.; Kerkhoven, R. M.; Madiredjo, M.; Nijkamp, W.; Weigelt, B.; Agami, R.; Ge, W.; Cavet, G.; Linsley, P. S.; Beijersbergen, R. L.; Bernards, R. A large-scale RNAi screen in human cells identifies new components of the p53 pathway. *Nature* **428:**431–437; 2004.

[12] Kolfschoten, I. G.; van Leeuwen, B.; Berns, K.; Mullenders, J.; Beijersbergen, R. L.; Bernards, R.; Voorhoeve, P. M.; Agami, R. A genetic screen identifies PITX1 as a suppressor of RAS activity and tumorigenicity. *Cell* **121:**849–858; 2005.

[13] Paddison, P. J.; Silva, J. M.; Conklin, D. S.; Schlabach, M.; Li, M.; Aruleba, S.; Balija, V.; O'Shaughnessy, A.; Gnoj, L.; Scobie, K.; Chang, K.; Westbrook, T.; Cleary, M.; Sachidanandam, R.; McCombie, W. R.; Elledge, S. J.; Hannon, G. J. A resource for large-scale RNA-interference-based screens in mammals. *Nature* **428:**427–431; 2004.

[14] Kargul, G. J.; Dudekula, D. B.; Qian, Y.; Lim, M. K.; Jaradat, S. A.; Tanaka, T. S.; Carter, M. G.; Ko, M. S. Verification and initial annotation of the NIA mouse 15K cDNA clone set. *Nat. Genet.* **28:**17–18; 2001.

[15] Haidara, K.; Morel, I.; Abalea, V.; Gascon Barre, M.; Denizeau, F. Mechanism of tert-butylhydroperoxide induced apoptosis in rat hepatocytes: involvement of mitochondria and endoplasmic reticulum. *Biochim. Biophys. Acta* **542:**173–185; 2002.

[16] Liu, H.; Miller, E.; van de Water, B.; Stevens, J. L. Endoplasmic reticulum stress proteins block oxidant-induced Ca2+ increases and cell death. *J. Biol. Chem.* **273:**12858–12862; 1998.

[17] Palomba, L.; Sestili, P.; Cantoni, O. tert-Butylhydroperoxide induces peroxynitrite-dependent mitochondrial permeability transition leading PC12 cells to necrosis. *J. Neurosci. Res.* **65:**387–395; 2001.

[18] Moise, A. R.; Kuksa, V.; Imanishi, Y.; Palczewski, K. Identification of all-trans-retinol:all-trans-13,14-dihydroretinol saturase. *J. Biol. Chem.* **279:** 50230–50242; 2004.

[19] Moise, A. R.; Kuksa, V.; Blaner, W. S.; Baehr, W.; Palczewski, K. Metabolism and transactivation activity of 13,14-dihydroretinoic acid. *J. Biol. Chem.* **280:**27815–27825; 2005.

[20] Kulms, D.; Schwarz, T. Molecular mechanisms involved in UV-induced apoptotic cell death. *Skin Pharmacol. Appl. Skin Physiol.* **15:**342–347; 2002.

[21] Han, J. F.; Wang, S. L.; He, X. Y.; Liu, C. Y.; Hong, J. Y. Effect of genetic variation on human cytochrome p450 reductase-mediated paraquat cytotoxicity. *Toxicol. Sci.* **91:**42–48; 2006.

[22] Dubuisson, M. L.; de Wergifosse, B.; Trouet, A.; Baguet, F.; Marchand-Brynaert, J.; Rees, J. F. Antioxidative properties of natural coelenterazine and synthetic methyl coelenterazine in rat hepatocytes subjected to tert-butyl hydroperoxide-induced oxidative stress. *Biochem. Pharmacol.* **60:**471–478; 2000.

[23] Piret, J. P.; Arnould, T.; Fuks, B.; Chatelain, P.; Remacle, J.; Michiels, C. Mitochondria permeability transition-dependent tert-butyl hydroperoxide-induced apoptosis in hepatoma HepG2 cells. *Biochem. Pharmacol.* **67:**611–620; 2004.

[24] Ryan, P. M.; Bedard, K.; Breining, T.; Cribb, A. E. Disruption of the endoplasmic reticulum by cytotoxins in LLC-PK1 cells. *Toxicol. Lett.* **159:**154–163; 2005.

[25] Monnier, V.; Girardot, F.; Audin, W.; Tricoire, H. Control of oxidative stress resistance by IP3 kinase in *Drosophila melanogaster*. *Free Radic. Biol. Med.* **33:**1250–1259; 2002.

[26] Cecchi, C.; Fiorillo, C.; Sorbi, S.; Latorraca, S.; Nacmias, B.; Bagnoli, S.; Nassi, P.; Liguri, G. Oxidative stress and reduced antioxidant defenses in peripheral cells from familial Alzheimer's patients. *Free Radic. Biol. Med.* **33:**1372–1379; 2002.

[27] Begni, B.; Brighina, L.; Sirtori, E.; Funagalli, L.; Andreoni, S.; Beretta, S.; Oster, T.; Malaplate-Armand, C.; Isella, V.; Appollonio, I.; Ferrarese, C. Oxidative stress impairs glutamate uptake in fibroblasts from patients with Alzheimer's disease. *Free Radic. Biol. Med.* **37:** 892–901; 2004.

[28] de Haan, J. B.; Cristiano, F.; Iannello, R.; Bladier, C.; Kelner, M. J.; Kola, I. Elevation in the ratio of Cu/Zn-superoxide dismutase to glutathione peroxidase activity induces features of cellular senescence and this effect is mediated by hydrogen peroxide. *Hum. Mol. Genet.* **5:** 283–292; 1996.

[29] Touyz, R. M.; Schiffren, E. L. Increased generation of superoxide by angiotensin II in smooth muscle cells from resistance arteries of hypertensive patients: role of phospholipase D-dependent NAD(P)H oxidase-sensitive pathways. *J. Hypertens.* **19:**1245–1254; 2001.

[30] Mendez, R.; Richter, J. D. Translational control by CPEB: a means to the end. *Nat. Rev. Mol. Cell Biol.* **2:**521–529; 2001.

[31] El Mouatassim, S.; Guerin, P.; Menezo, Y. Expression of genes encoding antioxidant enzymes in human and mouse oocytes during the final stages of maturation. *Mol. Hum. Reprod.* **5:**720–725; 1999.

[32] Park, E. J.; Kim, J. H.; Seong, R. H.; Kim, C. G.; Park, S. D.; Hong, S. H. Characterization of a novel mouse cDNA, ES18, involved in apoptotic cell death of T-cells. *Nucleic Acids Res.* **27:**1524–1530; 1999.